fire

MDPI

Article

Automated GC-FID Analysis of Brominated Flame Retardants in Polyester Resins with Hydrogen Carrier Gas

Nicola Mucci [1,2], Lorenzo Venturini [2], Niccolò Fanfani [2], Giovanni Cappelli [2], Ilaria Rapi [2,*], Donato Squillaci [2], Jacopo Ceccarelli [3], Antonio Baldassarre [1,2], Veronica Traversini [1,2] and Stefano Dugheri [4]

1 Division of Occupational Medicine, Careggi University Hospital, 50134 Florence, Italy; nicola.mucci@unifi.it (N.M.); antonio.baldassarre@unifi.it (A.B.); veronica.traversini@unifi.it (V.T.)
2 Department of Experimental and Clinical Medicine, University of Florence, 50134 Florence, Italy; lorenzo.venturini@unifi.it (L.V.); niccolo.fanfani@unifi.it (N.F.); giovanni.cappelli@unifi.it (G.C.); donato.squillaci@unifi.it (D.S.)
3 Intertek Italia S.p.A., 50055 Lastra a Signa, Italy; jacopo.ceccarelli@intertek.com
4 Department of Life Sciences, Health and Health Professions, Link Campus University, 00165 Rome, Italy; s.dugheri@unilink.it
* Correspondence: ilaria.rapi@unifi.it

Abstract: Brominated flame retardants (BFRs), including tetrabromobisphenol A (TBBPA) and dibromoneopentyl glycol (DBNPG), are present in both saturated and unsaturated polyester resins (UPRs). Given their toxicity, it is imperative to assess the content of this group of chemicals to ensure product safety and environmental sustainability, considering the paucity in the literature of analytical methods to evaluate them, particularly in solid matrices as UPRs. This study aimed to develop a fully automated gas chromatographic analysis of these BFRs, utilizing a flame ionization detector (FID), with prior derivatization of TBBPA and DBNPG with acetic anhydride. A chemometric evaluation was conducted for the derivatization step to enhance the yield of the procedure. The optimized method met the desired requirements for specificity, accuracy, and sensitivity, showing limits of detection (LOD) and quantitation (LOQ), respectively, of 1.1 µg/mL and 3.3 µg/mL for DBNPG and 3.6 µg/mL and 10.8 µg/mL for TBBPA. Other conventional detectors, i.e., an Electron Capture Detector (ECD) and a Mass Spectrometer (MS), were tested. The ECD showed a higher sensitivity than the FID and MS; however, its linearity proved to be more limited, making it unsuitable for higher concentration scenarios. The MS detector yielded results comparable with those of the FID, yet the latter is a cheaper and more sensitive alternative.

Keywords: brominated flame retardants; automated sample preparation; unsaturated polyester resins; GC-FID; micro-bore column

check for updates

Academic Editor: Grant Williamson

Received: 15 January 2025
Revised: 14 February 2025
Accepted: 17 February 2025
Published: 19 February 2025

Citation: Mucci, N.; Venturini, L.; Fanfani, N.; Cappelli, G.; Rapi, I.; Squillaci, D.; Ceccarelli, J.; Baldassarre, A.; Traversini, V.; Dugheri, S. Automated GC-FID Analysis of Brominated Flame Retardants in Polyester Resins with Hydrogen Carrier Gas. *Fire* **2025**, *8*, 82. https://doi.org/10.3390/fire8020082

Copyright: © 2025 by the authors. Licensee MDPI, Basel, Switzerland. This article is an open access article distributed under the terms and conditions of the Creative Commons Attribution (CC BY) license (https://creativecommons.org/licenses/by/4.0/).

1. Introduction

Tetrabromobisphenol A (TBBPA) and dibromoneopentyl glycol (DBNPG) are brominated flame retardants (BFRs) industrially added to polymeric products to reduce their flammability [1]. TBBPA, produced by the bromination of bisphenol A, is one of the most widely used BFRs [2] for the production of polyester, epoxy, phenolic, and acrylonitrile-butadiene–styrene resins [3]. The polymer resins play a crucial role in the market due to their versatility, durability, and wide range of applications (ranging from packaging materials to automotive components), serving as the backbone for countless products we encounter daily. In 2022, the global TBBPA market was estimated at 1100 million USD, and for the forecast period 2023–2029 is predicted to grow at a Compound Annual Growth Rate

(CAGR) of 3.0% to reach 1356.2 million USD [4]. However, the presence of brominated flame retardants in polymer resins has become a growing concern for product safety and environmental sustainability: norms provide guidelines for manufacturing processes and material properties, ensuring that polymer resins adhere to rigorous performance and safety standards [5]. TBBPA has low acute toxicity, being neither an irritant nor a skin sensitizer, but it affects the thyroid function, and it may also cause cancer in humans [3]. DBNPG is used primarily for the manufacturing of unsaturated polyester and epoxydic resins [6], and it is produced by substitution with bromine of the hydroxylic groups of pentaerythritol [7]. Exposure to DBNPG can cause eye and skin irritation, and the International Agency for Research on Cancer (IARC) classified it as "possibly carcinogenic to humans" (group 2B) [8]. Generally, during the process of combustion, the flame retardant decomposes at elevated temperatures releasing increasing volumes of non-combustible gas, thereby leading to a gradual reduction in the concentration of combustible gas and, hence, preventing the continuous combustion process [9]. The wide diffusion of BFRs in a variety of settings, including air, dust, food, drinking water, and indoor environments, has led to instances of human exposure throughout the lifecycle of BFR-containing products, from their production to their eventual disposal [10,11]. It is important to note that children may be particularly vulnerable due to their behaviors, such as crawling and mouthing objects [12]. Several BFR compounds, including persistent, bioaccumulative, and toxic (PBT) substances, have been detected in aquatic and terrestrial ecosystems. These compounds enter the environment through atmospheric transport, wastewater discharge, and surface runoff, which poses global ecological risks [13–16]. Given these premises, since the BFRs are widely applied in industry and can pose a health hazard, their presence in manufactured or semi-finished products is regulated by institutions. The European Union received the Globally Harmonized System of Classification and Labeling of Chemicals (GHS) with the promulgation of the Regulation (EC) No 1272/2008, commonly known as the CLP Regulation (Classification, Labeling, and Packaging), imposing 1000 ppm (0.1%) as the content limit in mixtures for TBBPA and DBNPG [17]. In the United States, the document HCS/HazCom 2012, promulgated by the Occupational Safety and Health Administration (OSHA), implemented the GHS and established the same limit for TBBPA and DBNGP [18]. Because unsaturated polyester resins (UPR) are usually present in a mixture with several other compounds, chromatographic separation methods such as Gas Chromatography (GC) or Liquid Chromatography (LC) might be suitable for their characterization, although there are still few studies on the subject [19–22]. According to our knowledge, methods are available in the literature for the analysis of TBBPA and DBNPG via GC and LC, mainly applied to environmental matrices for pollution analysis [2,23–29]. The use of chromatographic methods is encouraged in the field of the Green Analytical Chemistry (GAC) thanks to the possibility of multi-analyte methods [30]. Although derivatization is generally not suggested, miniaturization of the procedure results in a minimal use of hazardous substances, meeting the standard of GAC in terms of operator exposure and environmental impact. While functionalization is generally not needed for LC-MS analysis [31], the majority of the available works found in the literature use it as well as dedicated instrumental configurations [2,25–27,32]. In this context, a new miniaturized method for the analysis of these BFRs in organic media, such as semi-finished products like unsaturated polyester resin before the gelling process, would be suitable. The aim of this work was to propose an innovative, miniaturized, and fully automated method for the analysis of TBBPA and DBNPG through direct GC-FID injection, prepared by derivatization through reduced quantities of reagents (acetic anhydride, to obtain diacetyl derivatives). The derivatization process was optimized thanks to the chemometric design of the experiments and data evaluation. Chromatographic aspects and analytical performances,

along with a comparison of the performances with other conventional gas chromatographic detectors, to limit the costs and to save resources, were also discussed. To the best of our knowledge, there are no existent works in the literature concerning the quantification of these BFRs in UPR. This underscores the importance of a new analytical approach to verify compliance with international regulations before the marketing step of said products.

2. Materials and Methods

2.1. Chemicals and Reagents

3,3′,5,5′-tetrabromobisphenol A 97% (TBBPA) (CAS 79-94-7), dibromoneopentyl glycol 98% (DBNPG) (CAS 3296-90-0), acetic anhydride ≥ 99% (CAS 108-24-7), 4-bromophenol (4BP) 99% (CAS 106-41-2), hexane ≥ 99.5% (CAS 110-54-3), pyridine 99% (CAS 110-86-1), dichloromethane ≥ 99.9% (CAS 75-09-2), and sodium bicarbonate ≥ 99.5% (CAS 144-55-8) were purchased from Sigma-Aldrich (Saint Louis, MO, USA). The high purity hydrogen (>99.99999%) was generated in situ by a WM H2 desk generator (MicroPROGEL, Padova, Italy); bottled nitrogen (99.999%) and air (99.999%) were obtained from Nippon Gases-Rivoira (Turin, Italy).

2.2. Sample Preparation

For the determination of TBBPA and DBNPG, 500 mg of an unsaturated polyester resin sample was weighted in a 4 mL vial and dissolved with 500 µL of DCM. Then, 200 µL of pyridine, 20 µL of internal standard acetone solution (4BP, 10 mg/mL), and 100 µL of acetic anhydride were added. The mixture was heated for 2 h at 60 °C and then cooled to room temperature. To remove the excess of unreacted acetic anhydride, 1 mL of saturated $NaHCO_3$ water solution was added and the vial was vigorously stirred for 5 min (or until the end of effervescence). Then, 1 mL of hexane was added and the vial was stirred for liquid–liquid extraction. After the separation, 100 µL of organic extract was transferred to another 2 mL GC vial, containing 900 µL of hexane; 0.5 µL of the diluted solution was injected in the GC port.

2.3. Instrumental Conditions: GC-FID, GC-ECD, and GC-MS

An Agilent 7820A GC (Santa Clara, CA, USA) with a split/splitless injector and FID detector running on hydrogen carrier gas and micro-bore columns was operated as follows. The injector was used at 280 °C in split mode with a 1:50 split ratio, using a split liner with wool and UltraInert septa. The oven was set to initially maintain 60 °C for 1 min, then 30 °C/min to 300 °C with a 2 min hold, with a total run time of 12 min. The column was a micro-bore Supelco SLB-5ms 10 m × 100 µm I.D. × 0.1 µm (Merck KGaA, Darmstadt, Germany) with a set hydrogen flow of 0.47 mL/min (55 cm/s of linear velocity). The detector was kept at 360 °C with a fuel flow of 30 mL/min, air flow of 300 mL/min, N_2 makeup flow of 30 mL/min, and 20 Hz data acquisition. Also, a Varian CP3800 GC-ECD system, with 1079 injectors (SCION Instruments NL BV, Amundsenweg, The Netherlands), was used. The injection was carried out in split mode (1:50, injection temperature 250 °C). The chromatographic column was an Agilent J&W DB 35-MS-UI GC Column (30 m × 0.25 mm, 0.25 µm). The instrument was coupled with Varian ^{63}Ni ECD. The initial column temperature was set to 50 °C (1 min) and then increased by 10 °C/min to 260 °C (total run time of 22 min). Helium, as the carrier gas, and Ar-CH_4, as the gas makeup, were used and set at 2.0 mL/min and 30 mL/min, respectively. For spectral confirmation, an Agilent 7890B GC was coupled with a mass spectrometer Agilent 7000D triple quadrupole. The injection was carried out in split mode (1:20) and with the injector temperature set at 280 °C. The chromatographic column was a J&W VF5-ms (30 m × 250 µm I.D. × 0.25 µm). The initial temperature column was set to 60 °C (0.5 min)

and then increased by 15 °C/min to 320 °C, held for 5 min (total run time of 23 min). The carrier gas was helium, set at 1.3 mL/min. The m/z acquisition window in scan mode was 50–650 m/z.

2.4. Experimental Design

In order to optimize the analytical method in terms of the derivatization, three factors were studied in two levels each, so a 2^3 full factorial design was performed. The first factor (x_1) was the volume of pyridine used as a solvent in the derivatization step (50–500 µL). The second one (x_2) was the volume of acetic anhydride used as a derivatizing agent (20–100 µL). The last (x_3) was the time of reaction (30–360 min). As shown in Table 1, only 8 experiments were performed, in triplicate, to optimize the method, while two more experiments (C1 and C2) were used to validate the models.

Table 1. The experiments performed to optimize the method and the experimental matrix with the corresponding experimental plan.

	Experimental Matrix			**Experimental Plan**		
Exp#	**x_1**	**x_2**	**x_3**	**Volume of Pyridine (µL)**	**Volume of Acetic Anhydride (µL)**	**Time of Reaction (min)**
1	−1	−1	−1	50	20	30
2	1	−1	−1	500	20	30
3	−1	1	−1	50	100	30
4	1	1	−1	500	100	30
5	−1	−1	1	50	20	360
6	1	−1	1	500	20	360
7	−1	1	1	50	100	360
8	1	1	1	500	100	360
C1	−0.3	1	−1	200	100	30
C2	−0.8	−0.2	1	100	50	360

The aim of this study was to maximize the sensitivity of the method for the two analytes of interest (DBNPG and TBBPA), so the experimental design was applied to maximize the responses, in terms of peak areas, of the di-acetylated products. Microsoft Excel (Version 6.0) was used to collect data, while Chemometric Agile Tool (CAT, Version 1.0), an open source and R-based software [33], was used to process it.

2.5. Online Robotic System

Automation of the analytical procedure was achieved using the Gerstel MultiPurpose Sampler (MPS) robotic DualHead Smart Series Autosampler (Figure 1). The apparatus was equipped with a variety of instrumental parts that enhance its capabilities and efficiency in sample handling and automated sample preparation. Among these, a syringe detection system, a 120 cm x-axis to ensure extensive coverage, and two robotic injection units for optimal flexibility in analysis execution were utilized. To further streamline operations, an offline Toolstation was used, while a Decapper module allowed for the opening and closing of initially sealed vials with the option to use appropriate caps for multiple operations. The QuickMix system enabled extremely rapid and efficient sample agitation, while an MPS smart liquid injection kit included a wash station, a tray holder, and a universal syringe module. Additionally, modules for agitation, washing, and solvent preparation were present, along with various tray options for vials of different sizes. The entire system was controlled via the MAESTRO basic software (Version 1.4.59.4), which provides sample

control and preparation functions. This setup enables a higher throughput, with a reduced exposure for the operator and a general reduction in analytical errors.

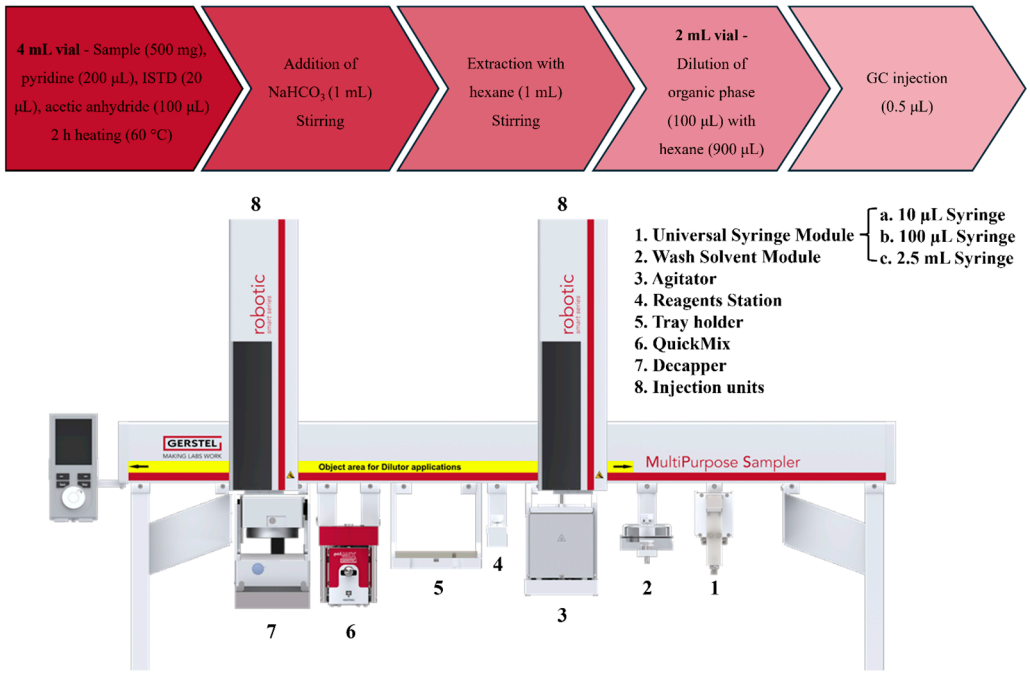


Figure 1. Flow chart and image of autosampler for the fully automated on-sample derivatization and analysis of TBBPA and DBNPG.

2.6. Calibration Curve Construction

The standard solution (5 mg/mL) and internal standard solution (10 mg/mL) were prepared by dissolving the analytes (50 mg) in the proper acetone volume. A working solution (2.5 mg/mL) was prepared mixing equal volumes of DBNPG and TBBPA standard solutions. Points at different concentrations were prepared by dilution from the working solution, dispensing proper volumes in 4 mL vials, containing DCM (500 µL) and ISTD solution (20 µL). Then, pyridine (200 µL), acetic anhydride (100 µL), and saturated $NaHCO_3$ (1 mL) were added, obtaining a concentration from 5 to 100 µg/mL. The calibration solutions were then treated as described in Section 2.2.

2.7. Method Performance Evaluation

To assess the accuracy and the precision of the method, two control solutions (25 and 75 µg/mL) were prepared using the procedure described above and analyzed with GC-FID. Calibration curves were obtained plotting the peak area of the di-acetylated BFR versus the nominal concentration of each calibration solution, attaining a least-square linear regression as the best fitting function. Limit of Detection (LOD) and Limit of Quantitation (LOQ) values were determined by the standard deviation (SD) of the response and slope approach. In fact, the value of the LOD was strongly influenced by the stability and reproducibility of the background noise, when the LOD was checked as a signal-to-noise (S/N) evaluation approach. Therefore, by the standard deviation of the Y-intercepts (SDY-I) of the regression curves, it was possible to calculate the estimated SDs of the responses. The Relative Standard Deviation (RSD%) approach was used to evaluate the precision of the quantitative data of the replicate analysis of the control solution. The calculation of the yield between the determined and nominal amounts of the control solution permitted the determination of the accuracy.

3. Results

To approach the gas chromatographic quantification of free BFRs in organic media, multiple instrumental configurations were evaluated. The GC equipped with a Flame Ionization Detector (FID) was selected for its sensitivity, roughness, and broad availability in quality control and production laboratories. To enhance the analytical productivity and reduce the environmental footprint of the determination, hydrogen as a carrier gas and microbore columns were applied [34], since helium has recently undergone repeated periods of shortage at a global level and presented difficulties among the supply chain [1–3,35–37]. The adoption of hydrogen as a carrier permits a reduction in analysis cycle times of up to 30%, while maintaining similar conditions to He-supplied columns [38–40]. Hydrogen is the carrier gas with the lowest density and viscosity, allowing lower head pressure to reach the needed flow rates. The conjunction of hydrogen and the micro-bore columns (0.10–0.20 mm I.D.) greatly enhances the laboratory productivity, while maintaining or improving the separation efficiency using shorter columns [41].

3.1. Derivatization Optimization

In order to perform the analysis of TBBPA and DBNPG via GC, the derivatization step is crucial (Figures 2 and 3). Various viable alternatives can be found in the literature concerning the derivatization of hydroxyl groups, such as methylation or acetylation [42,43]; nonetheless, the use of hazardous reagents such as trimethyloxonium tetrafluoroborate (TMO), widely used in the past, is not compliant with GAC principles and should thus be replaced. Acetic anhydride was chosen as the derivatizing agent for the present work due to its cost-effectiveness and easy availability. Additionally, acetic anhydride has recently been positioned between "recommended" and "problematic" in terms of environmental friendliness, implying a degree of acceptance for its use in small quantities [44]: in our opinion, utilizing 100 µL per sample presents a favorable compromise.

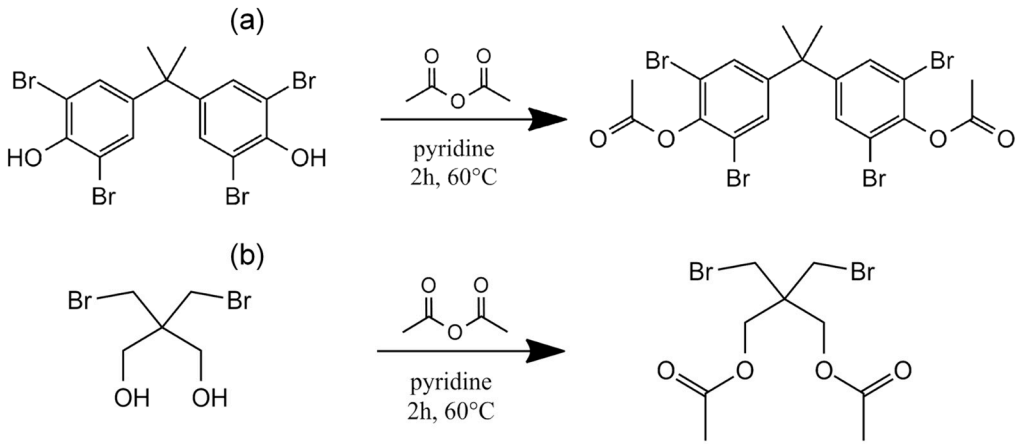


Figure 2. Functionalization of TBBPA (**a**) and DBNPG (**b**) with acetic anhydride.

A preliminary test was conducted on both TBBPA and DBNPG, dissolved in acetone, with the addition of acetic anhydride and heating for 30 min at 60 °C. After workup and injection in GC-MS, the analysis of the chromatograms evidenced that these conditions were suitable for TBBPA, but no reaction was observed for DBNPG. For this reason, different conditions were investigated. In the literature, the functionalization of DBNPG with acetic anhydride using pyridine as a solvent is reported as intermediate in the total synthesis of 2-bromomethyl-3-hydroxy-2-hydroxymethyl-propyl pyrimidine and theophylline nucleosides [45]. The use of pyridine as a catalytic environment for acetylation on difficult substrates has also been reported [46–48]. Preliminary GC-FID and GC-MS tests showed

an increase in the signal attributed to the di-acetylated DBNPG in the chromatogram. Subsequently, TBBPA was added to the mixture and the response was maintained. Figure 2 shows the derivatization reaction of both analytes.

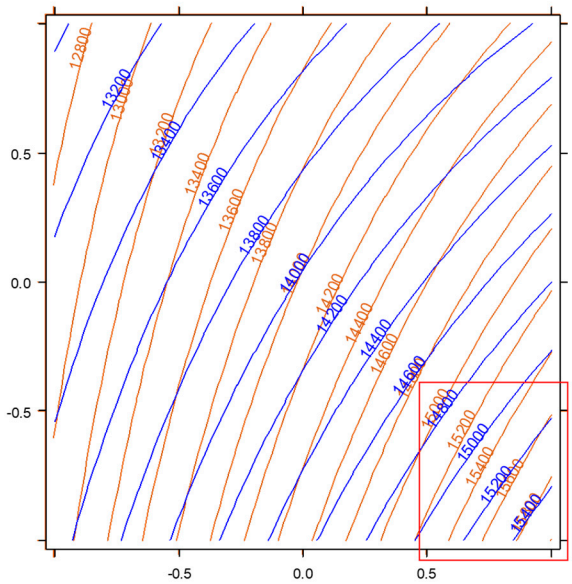


Figure 3. Overlapping of the contour plots obtained for the model describing the acetylated DBNPG (Y_1); in the y−axis, the factor x_3 is reported, while in the x−axis, the values for factor x_2 are reported in blue lines versus, in orange lines, the values for factor x_1. The optimal is squared in red.

The optimization of the derivatization conditions was conducted applying the 2^3 full factorial design as described in Table 1. Moreover, the models describing the sensitivity of the method were validated in two test points (C1 and C2) belonging to the experimental domain. The amounts of pyridine (50–500 µL) and acetic anhydride (20–100 µL) and different reaction times (30 min–6 h) were investigated in order to maximize the peak area of the di-acetylated products of DBNPG and TBBPA. The results clearly show that the studied models are similar (for the comparison between the obtained response surfaces, see the attached Supplementary Information, Figure S1), so the experimental conditions that allow for obtaining the highest sensitivity for DBNPG also optimize also the sensitivity for TBBPA.

In particular, it is evident that the increase in the reaction time decreases the yield of the di-acetylated products, while the highest sensitivities are reached when the volumes of both the solvent and derivatization reagent are high. So, as can be seen in Figures 3 and 4, the analysis of the models demonstrates that the optimal experimental conditions to perform the derivatization of the two analytes are obtained working with 500 µL of pyridine ($x_1 = 1$), 100 µL of acetic anhydride ($x_2 = 1$), and 30 min as the reaction time ($x_3 = -1$).

Because the predicted responses are not significantly different from the experimental ones, the two models describing the sensitivity of DBNPG (Y1) and of TBBPA (Y2) were validated at the test points (C1 and C2 in Table 1) with a confidence interval of 95%.

Once the derivatization procedure was optimized, a test for the selection of the internal standard was performed. Since DBNPG is used with neopentyl glycol in polymeric formulations, the latter glycol cannot be used because it might already be present in the mixture. In order to trace the results of the reaction, a known and constant amount of 4-bromophenol was added, and the response of the acetylated derivative was used as the internal standard (Figure 5).

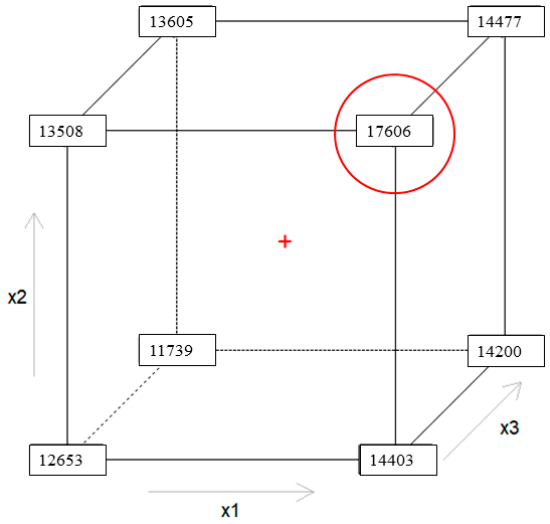


Figure 4. Experimental domain with the peak area intensities obtained in each experiment for the di-acetylated DBNPG: it is highlighted in red in experiment number 4, which allows for obtaining the highest sensibility (the model for the di-acetylated TBBPA is not reported, as it is equal to this one).

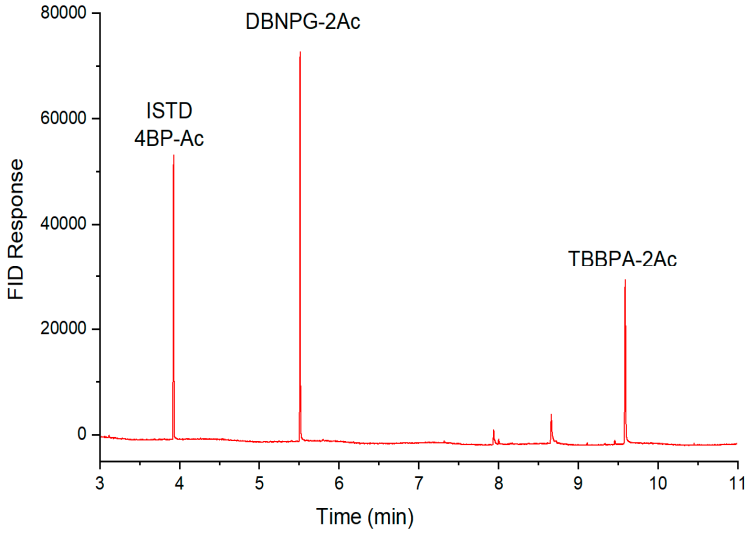


Figure 5. FID-Chromatogram of 4-bromophenol (4BP), dibromoneopenthyl glycol (DBNPG), and tetrabromobisphenol A (TBBPA), fully acetylated (DBNPG−2Ac and TBBPA−2Ac, respectively).

During the optimization procedure, some experiments led to the formation of multiple peaks for the targeted BFRs; in particular, TBBPA showed the chromatographic separation of three peaks (Figure 6). After GC-MS analysis, the three peaks were explained by the incomplete yield of the derivatization reaction (Figure 7): the obtained EI mass spectra confirmed the first eluting peak as the underivatized BFR and the subsequent ones as mono- and bi-acetylated derivatives, respectively (Figures S2–S4). Mass spectra for acetylated TBBPA and DBNPG were not found in the literature, but the fragmentation pattern and isotopic distribution of polybrominated compounds confirmed the hypothesized structures. In the spectra of TBBPA acetylation products, the intensity ratios of the major fragmentation pattern clearly changed, in addition to the appearance of peaks at a higher m/z ratio (Figure S4). For DBNPG, the formation of mono-acetylated products was not observed.

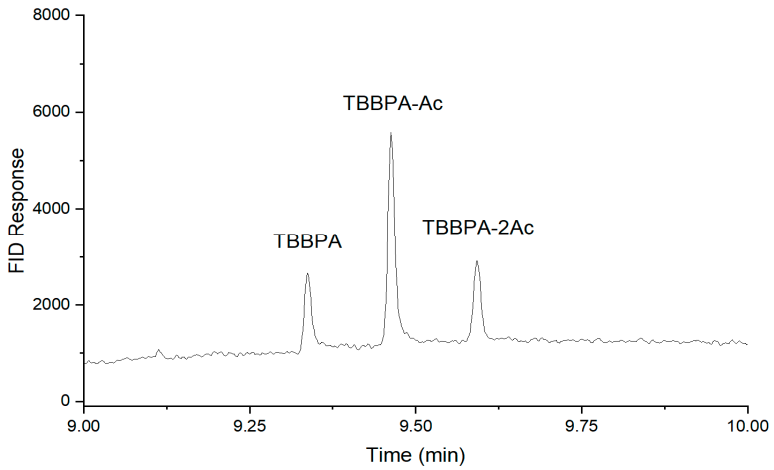


Figure 6. FID−Chromatogram of tetrabromobisphenol A (TBBPA), mono-acetylated tetrabromobisphenol A (TBBPA−Ac), bi-acetylated tetrabromobisphenol A (TBBPA−2Ac).

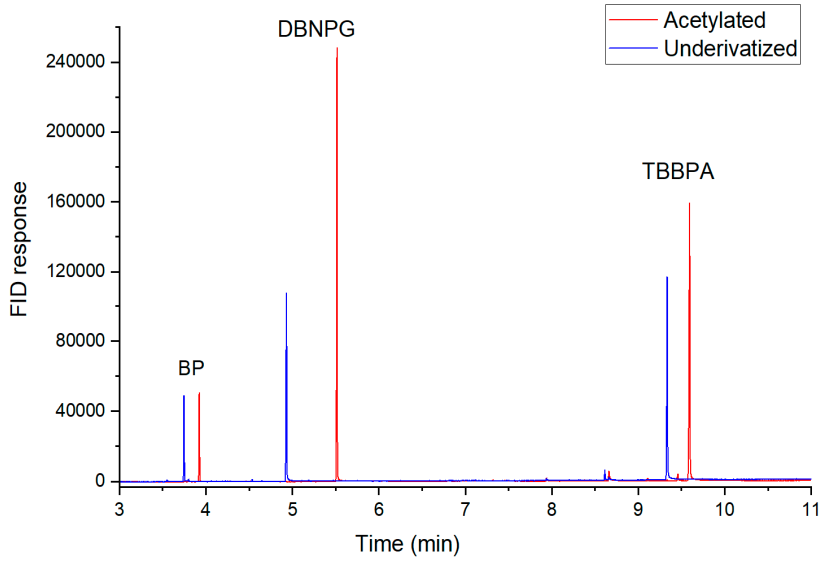


Figure 7. FID−Chromatogram of internal standard and analytes in acetylated and underivatized conditions.

These findings allowed for adding a degree of confirmation of the derivatization reaction, since possible issues in derivatization completion can be traced by monitoring the presence of unreacted analytes.

3.2. Performance Results Assessment

In Table 2, the Limit of Detection (LOD), Limit of Quantitation (LOQ), Relative Standard Deviation (RSD %), Accuracy (Acc %), and R^2 of the regression curve are reported. The RSD (%) was calculated as the standard deviation of the control point divided by its average value, while the Acc (%) was calculated by the average value divided by the nominal value. The RSD (%) and Acc (%) were evaluated using a low curve point and a high curve point, corresponding to 25 µg/mL and 75 µg/mL, respectively. The LOD was calculated by multiplying 3.3 by the ratio between the standard deviation of the Y-intercept and the slope of the average daily curve, and the LOQ is three times the LOD according to ICH guidelines [49].

Table 2. Performance evaluation of the method with FID detector.

BFR	LOD (µg/mL)	LOQ (µg/mL)	RSD (n = 5)		Acc (%)		R^2
			25 µg/mL	75 µg/mL	25 µg/mL	75 µg/mL	
DBNPG	1.1	3.3	1.9%	1.0%	94%	105%	0.998
BBPA	3.6	10.8	2.6%	1.0%	93%	106%	0.998

Despite the direct injection of standard solutions of BFRs being proved to be viable, the injection of untreated viscous resins and diluted polymeric products could damage the instrument, compromising its integrity. Hence, examining in GC resins which have been previously extracted and derivatized creates less stress for the components of the instrument, therefore requiring less frequent maintenance. This approach not only safeguards the instrument's integrity but also enhances the accuracy and reliability of the analytical results.

The unavailability of BFR-free matrix to perform a calibration, which, when feasible, is generally considered the preferred option, necessitated the execution of an external curve approach. Compared to underivatized determination (Table S1), the use of acetic anhydride permitted lower detection limits, better repeatability, and an increase in the slope of the calibration curve of 116% for DBNPG and 23% for TBBPA. The improved repeatability and method roughness allowed for increasing the throughput without any operator intervention, maximizing the analytical productivity.

3.3. Comparison of Detector Performance

To provide an overview of sensitivity, robustness, greenness, specificity, and cost, we applied the method developed with the FID, ECD, and MS detector. We calculated the analytical parameters (LOD, LOQ, and R^2) as described in the performance result assessment. In the range of the investigated concentrations, the calibration curves showed excellent linearity and sensitivity, as shown in Table 3.

Table 3. Performance evaluation of the method with the FID, ECD, and MS detector.

BFR	FID				ECD				MS			
	LOD (µg/mL)	LOQ (µg/mL)	m	R^2	LOD (µg/mL)	LOQ (µg/mL)	m	R^2	LOD (µg/mL)	LOQ (µg/mL)	m	R^2
DBNPG	1.1	2.6	23,051	0.998	0.6	1.8	58,644	0.998	1.7	4.1	21,148	0.999
BBPA	3.6	4.5	22,163	0.998	1.6	3.1	54,319	0.997	5.0	7.9	19,927	0.998

The ECD detector exhibited the highest sensitivity, as defined by the slope of the equations, while the MS and FID showed slightly lower sensitivity. However, the LOD observed for the FID and MS are satisfactory for our experimental conditions. Nonetheless, despite the ECD demonstrating a greater sensitivity, it has a narrower range of linearity compared to the FID and MS: this may limit its applicability in certain scenarios, where the concentration exceeds the calibration presented in this work. In our opinion, the MS is the most suitable detector in the presence of a complex matrix, as it allows for the identification of other substances potentially present in the same chromatographic run. However, the use of other detectors is favored due to the high overall cost of the MS instrument and the requirement of highly trained operators. In fact, in this context, the FID is a cheaper alternative. Concerning the greenness, the use of the ECD is limited by the presence of the radioisotope ^{63}Ni, which leads to problems in terms of disposal, as well as safety. The necessity of pumping stages for the MS, which translates into higher maintenance costs,

makes the FID the best alternative, due to its reduced overall cost and consumption. In addition, the use of hard-to-manage gases like argon–methane, as well as hydrogen for the FID, could represent a safety problem for these detection systems. These considerations are presented in Figure 8, in which a numeric value, within the range of 1–10 (1–3 for regular, 4–7 for discrete, and 8–10 for very high), was assigned to each of the five parameters discussed above.

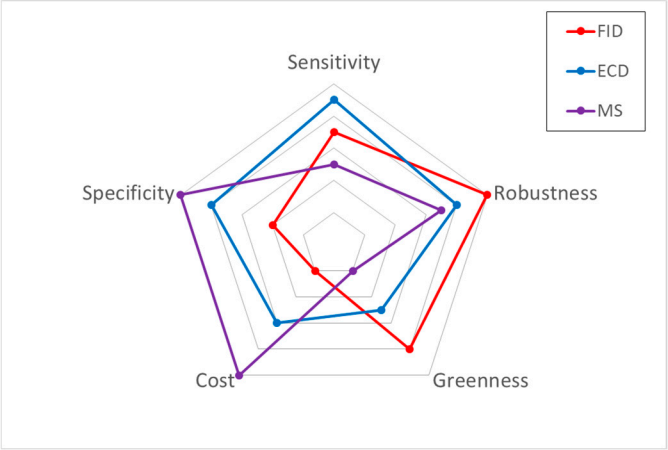


Figure 8. Radar chart detector comparison.

Generally, the sensitivities obtained exploiting the three detectors surveyed can be considered in line with other results present in the literature. However, depending on the matrix investigated and the analytical setup used, the outcome is very broad, ranging from ppt to ppm [29,50–54].

4. Conclusions

The analytical method developed in this study has proved to be suitable to test the content of BFRs in saturated and unsaturated polyester resins. The use of hydrogen and micro-bore GC columns led to a rapid and well-resolute chromatographic separation, while the pairing of a FID detector and the optimized derivatization with acetic anhydride resulted in a suitable sensitivity, capable of assessing the BFR content in preformed and finished polymeric products.

Supplementary Materials: The following supporting information can be downloaded at: https://www.mdpi.com/article/10.3390/fire8020082/s1, Figure S1: Comparison between the response surfaces obtained for the model describing the peak area of the acetylated DBNPG (panels 1A, 1B, and 1C) and for the one describing the peak area of the acetylated TBBPA (panels 2A, 2B, and 2C); Figure S2: EI Mass spectra of non-derivatized (a) and derivatized (b) DBNPG; Figure S3: Detail on molecular ion of derivatized DBNPG; Figure S4: EI Mass spectra of (a) tetrabromobisphenol A (TBBPA), (b) mono-acetylated tetrabromobisphenol A (TBBPA-Ac), (c) bi-acetylated tetrabromobisphenol A (TBBPA-2Ac); Table S1: Performance evaluation of the method without derivatization on standard mixtures.

Author Contributions: Conceptualization, N.M. and L.V.; methodology, N.F., G.C. and I.R.; software, D.S.; validation, L.V., G.C. and I.R.; formal analysis, L.V. and N.F.; investigation, D.S.; resources, J.C.; data curation, J.C.; writing—original draft preparation, S.D. and G.C.; writing—review and editing, A.B. and V.T.; supervision, S.D.; project administration, S.D. All authors have read and agreed to the published version of the manuscript.

Funding: This research received no external funding.

Institutional Review Board Statement: Not applicable.

Informed Consent Statement: Not applicable.

Data Availability Statement: The original contributions presented in this study are included in the article/Supplementary Material. Further inquiries can be directed to the corresponding author.

Acknowledgments: We thank Polynt S.p.A. (San Giovanni Valdarno, Arezzo, Italy), one of the world's largest manufacturers and suppliers of polyester gel coats, for allowing us access to their laboratories, and we thank their employees, particularly Alessandro Renzi, for enduring our presence and participating in the study.

Conflicts of Interest: Author Jacopo Ceccarelli was employed by the company Intertek Italia S.p.A. The remaining authors declare that the research was conducted in the absence of any commercial or financial relationships that could be construed as a potential conflict of interest.

References

1. European Food Safety Authority (EFSA). Brominated Flame Retardants. Available online: https://www.efsa.europa.eu/en/topics/topic/brominated-flame-retardants (accessed on 20 May 2024).
2. Xie, Z.; Ebinghaus, R.; Lohmann, R.; Heemken, O.; Caba, A.; Püttmann, W. Trace Determination of the Flame Retardant Tetrabromobisphenol A in the Atmosphere by Gas Chromatography–Mass Spectrometry. *Anal. Chim. Acta* **2007**, *584*, 333–342. [CrossRef] [PubMed]
3. Department of Health. Australian Government. Tetrabromobisphenol A (National Industrial Chemicals Notification and Assessment Scheme). Available online: https://www.industrialchemicals.gov.au/sites/default/files/2021-06/PEC42-Tetrabromobisphenol-A-TBBPA_0.pdf (accessed on 20 May 2024).
4. Market.us. Global Tetrabromobisphenol-A (Tbba) (Cas 79-94-7) Market by Type (Tablet, Oral Solution, Capsule), by Function (Intermediate, Plastic Housings, PCB or Laminates, Others), by Application (Transfusional Iron Overload, NTDT Caused Iron Overload), By Region and Key Companies - Industry Segment Outlook, Market Assessment, Competition Scenario, Trends and Forecast 2024–2033. Available online: https://market.us/report/tetrabromobisphenol-a-tbba-cas-79-94-7-market/#requestSample (accessed on 20 May 2024).
5. European Chemicals Agency (ECHA). Proposal for Identification of a Substance of Very High Concern on the Basis of the Criteria Set Out in REACH Article 57. 2022. Available online: https://echa.europa.eu/documents/10162/7a28f148-5576-a7d3-8236-10c718abc52f (accessed on 20 May 2024).
6. Vilcea, E.J.; Ion, R.M. Aspects of Flame Retardants and Their Role In Society, (National Scientific Session of the Academy of Romanian Scientists). Available online: https://www.aos.ro/wp-content/proceedings/PVol1Nr2Art.15.pdf (accessed on 20 May 2024).
7. National Center for Biotechnology Information. PubChem Compound Summary for CID 18692, 2,2-Bis(Bromomethyl)-1,3-Propanediol. Available online: https://pubchem.ncbi.nlm.nih.gov/compound/2_2-Bis_bromomethyl_-1_3-propanediol (accessed on 20 May 2024).
8. World Health Organization International Agency for Research on Cancer (IARC). *IARC Monographs on the Evaluation of Carcinogenic Risks to Humans*; IARC: Lyon, France, 2000.
9. Shen, J.; Liang, J.; Lin, X.; Lin, H.; Yu, J.; Wang, S. The Flame-Retardant Mechanisms and Preparation of Polymer Composites and Their Potential Application in Construction Engineering. *Polymers* **2021**, *14*, 82. [CrossRef] [PubMed]
10. Abdallah, M.A.-E.; Harrad, S. Dermal Uptake of chlorinated Organophosphate Flame Retardants via contact with Furniture Fabrics; implications for human exposure. *Environ. Res.* **2022**, *209*, 112847. [CrossRef]
11. Page, J.; Whaley, P.; Bellingham, M.; Birnbaum, L.S.; Cavoski, A.; Dilke, D.F.; Garside, R.; Harrad, S.; Kelly, F.; Kortenkamp, A.; et al. A New consensus on Reconciling Fire safety with environmental & health impacts of Flame Retardants. *Environ. Int.* **2023**, *173*, 107782. [CrossRef] [PubMed]
12. Sugeng, E.J.; De Cock, M.; Leonards, P.E.G.; Van deBor, M. Toddler Behavior, the home environment, and Flame Retardant exposure. *Chemosphere* **2020**, *252*, 126588. [CrossRef]
13. Ekpe, O.D.; Choo, G.; Barceló, D.; Oh, J.E. Introduction of emerging halogenated Flame Retardants in the environment. *Compr. Anal. Chem.* **2020**, *88*, 1–39. [CrossRef]
14. Brommer, S.; Harrad, S. Sources and humanexposure implications of concentrations of Organophosphate Flame Retardants in Dust from UK cars, classrooms, living Rooms, and Offices. *Environ. Int.* **2015**, *83*, 202–207. [CrossRef] [PubMed]
15. Yao, C.; Yang, H.; Li, Y. A Review on Organophosphate Flame Retardants in the environment: Occurrence, accumulation, Metabolism and toxicity. *Sci. Total Environ.* **2021**, *795*, 148837. [CrossRef] [PubMed]

16. ECHA Raises Environmental Concerns Over Certain Aromatic Brominated Flame Retardants. Available online: https://echa.europa.eu/it/-/echa-raises-environmental-concerns-over-certain-aromatic-brominated-flame-retardants (accessed on 10 February 2025).
17. EUR-Lex. Regulation (EC) No 1272/2008. Available online: https://eur-lex.europa.eu/legal-content/IT/TXT/?uri=celex:32008R1272 (accessed on 20 May 2024).
18. Hazard Communication—HCS/HazCom 2012 Final Rule & Appendices (United States Department of Labor). Available online: https://www.osha.gov/hazcom/ghs-final-rule (accessed on 20 May 2024).
19. BïÇen, A.; Güvenç, N. The Identification and Characterization of Unsaturated Polyester Resins Used in the Coating Industry/Boya Endüstrisinde Kullanılan Doymamış Polyester Reçinelerin Belirlenmesi ve Karakterizasyonu. *Erzincan Üniversitesi Fen Bilim. Enstitüsü Derg.* **2021**, *14*, 1077–1086. [CrossRef]
20. Ceccarelli, J.; Dugheri, S.; Cappelli, G.; Fanfani, N.; Squillaci, D.; Bucaletti, E.; Mucci, N.; Arcangeli, G. Simultaneous Determination by Selective Esterification of Trimellitic, Phthalic, and Maleic Anhydrides in the Presence of Respective Acids. *ACS Omega* **2023**, *8*, 15397–15405. [CrossRef] [PubMed]
21. Dugheri, S.; Bonari, A.; Pompilio, I.; Mucci, N.; Montalti, M.; Arcangeli, G. Development of new gas chromatography/mass spectrometry procedure for the determination of hexahydrophthalic anhydride in unsaturated polyester resins. *Rasayan J. Chem.* **2016**, *9*, 657–666.
22. Dugheri, S.; Marrubini, G.; Speltini, A.; Mucci, N.; Cappelli, G.; Bartolucci, G.; Arcangeli, G. Fully Automated Determination of Trimellitic Anhydride in Saturated Polyester Resins Using Programmed Temperature Vaporization-Large Volume Injection-Gas Chromatography Previous Aqueous Derivatization with Triethyloxonium Tetrafluoroborate. *Chromatographia* **2020**, *83*, 601–613. [CrossRef]
23. Sellström, U.; Jansson, B. Analysis of Tetrabromobisphenol A in a Product and Environmental Samples. *Chemosphere* **1995**, *31*, 3085–3092. [CrossRef]
24. Polo, M.; Llompart, M.; Garcia-Jares, C.; Gomez-Noya, G.; Bollain, M.-H.; Cela, R. Development of a Solid-Phase Microextraction Method for the Analysis of Phenolic Flame Retardants in Water Samples. *J. Chromatogr. A* **2006**, *1124*, 11–21. [CrossRef]
25. Frederiksen, M.; Vorkamp, K.; Bossi, R.; Rigét, F.; Dam, M.; Svensmark, B. Method Development for Simultaneous Analysis of HBCD, TBBPA, and Dimethyl-TBBPA in Marine Biota from Greenland and the Faroe Islands. *Int. J. Environ. Anal. Chem.* **2007**, *87*, 1095–1109. [CrossRef]
26. Dirtu, A.C.; Roosens, L.; Geens, T.; Gheorghe, A.; Neels, H.; Covaci, A. Simultaneous Determination of Bisphenol A, Triclosan, and Tetrabromobisphenol A in Human Serum Using Solid-Phase Extraction and Gas Chromatography-Electron Capture Negative-Ionization Mass Spectrometry. *Anal. Bioanal. Chem.* **2008**, *391*, 1175–1181. [CrossRef] [PubMed]
27. Sánchez-Brunete, C.; Miguel, E.; Tadeo, J.L. Determination of Tetrabromobisphenol-A, Tetrachlorobisphenol-A and Bisphenol-A in Soil by Ultrasonic Assisted Extraction and Gas Chromatography–Mass Spectrometry. *J. Chromatogr. A* **2009**, *1216*, 5497–5503. [CrossRef]
28. Di Napoli-Davis, G.; Owens, J.E. Quantitation of Tetrabromobisphenol-A from Dust Sampled on Consumer Electronics by Dispersed Liquid-Liquid Microextraction. *Environ. Pollut.* **2013**, *180*, 274–280. [CrossRef] [PubMed]
29. Balaban, N.; Gelman, F.; Taylor, A.A.; Walker, S.L.; Bernstein, A.; Ronen, Z. Degradation of Brominated Organic Compounds (Flame Retardants) by a Four-Strain Consortium Isolated from Contaminated Groundwater. *Appl. Sci.* **2021**, *11*, 6263. [CrossRef]
30. Płotka-Wasylka, J.; Namieśnik, J. *Green Analytical Chemistry: Past, Present and Perspectives*; Springer: Berlin/Heidelberg, Germany, 2019.
31. Qu, G.; Liu, A.; Hu, L.; Liu, S.; Shi, J.; Jiang, G. Recent Advances in the Analysis of TBBPA/TBBPS, TBBPA/TBBPS Derivatives and Their Transformation Products. *TrAC Trends Anal. Chem.* **2016**, *83*, 14–24. [CrossRef]
32. Paseiro-Cerrato, R.; Ackerman, L.; De Jager, L.; Begley, T. Brominated Flame Retardants (BFRs) in Contaminated Food Contact Articles: Identification Using DART-HRMS and GC-MS. *Food Addit. Contam. Part A* **2021**, *38*, 350–359. [CrossRef] [PubMed]
33. Leardi, R.; Melzi, C.; Polotti, G. CAT (Chemometric Agile Tool). Available online: http://gruppochemiometria.it/index.php/software (accessed on 20 May 2024).
34. Maštovská, K.; Lehotay, S.J. Practical Approaches to Fast Gas Chromatography–Mass Spectrometry. *J. Chromatogr. A* **2003**, *1000*, 153–180. [CrossRef] [PubMed]
35. Taylor, T. Not Another Helium Crisis! Available online: https://www.chromatographyonline.com/view/-not-another-helium-crisis- (accessed on 20 May 2024).
36. Kramer, D. Helium Prices Surge to Record Levels as Shortage Continues. *Phys. Today* **2023**, *76*, 18–20. [CrossRef]
37. Spatolisano, E.; Pellegrini, L.A. Helium Shortage 4.0: How to Face the Problem Through Its Energy-Efficient Recovery from Natural Gas. *Chem. Eng. Trans.* **2023**, *100*, 565–570. [CrossRef]
38. Buse, J.; Robinson, J.L.; Shyne, R.; Chi, Q.; Affleck, D.; Duce, D.; Seiden-Long, I. Rising above helium: A hydrogen carrier gas chromatography flame ionization detection (GC-FID) method for the simultaneous quantification of toxic alcohols and ethylene glycol in human plasma specimens. *Clin. Biochem.* **2019**, *73*, 98–104. [CrossRef] [PubMed]

39. Cutillas, V.; García-Gallego, G.; Murcia-Morales, M.; Ferrer, C.; Fernández-Alba, A.R. Beyond helium: Hydrogen as a carrier gas in multiresidue pesticide analysis in fruits and vegetables by GC-MS/MS. *Anal. Methods* **2024**, *16*, 1564–1569. [CrossRef]
40. Galletta, M.; Zoccali, M.; Jones, N.; Mondello, L.; Tranchida, P.Q. Flow-modulated comprehensive two-dimensional gas chromatography combined with time-of-flight mass spectrometry: Use of hydrogen as a more sustainable alternative to helium. *Anal. Bioanal. Chem.* **2022**, *414*, 6371–6378. [CrossRef] [PubMed]
41. Taylor, T. Hydrogen Carrier Gas for Gas Chromatography Mass Spectrometry (GC–MS)—A Practical Guide. Available online: https://www.chromatographyonline.com/view/the-lcgc-blog-hydrogen-carrier-gas-for-gas-chromatography-mass-spectrometry-gc-ms-a-practical-guide (accessed on 20 May 2024).
42. Palacio Lozano, D.C.; Jones, H.E.; Barrow, M.P.; Wills, M. Chemoselective Derivatisation and Ultrahigh Resolution Mass Spectrometry for the Determination of Hydroxyl Functional Groups within Complex Bio-Oils. *RSC Adv.* **2023**, *13*, 17727–17741. [CrossRef] [PubMed]
43. Chericoni, S.; Battistini, I.; Dugheri, S.; Pacenti, M.; Giusiani, M. Novel Method for Simultaneous Aqueous in Situ Derivatization of THC and THC-COOH in Human Urine Samples: Validation and Application to Real Samples. *J. Anal. Toxicol.* **2011**, *35*, 193–198. [CrossRef] [PubMed]
44. Byrne, F.P.; Jin, S.; Paggiola, G.; Petchey, T.H.M.; Clark, J.H.; Farmer, T.J.; Hunt, A.J.; Robert McElroy, C.; Sherwood, J. Tools and Techniques for Solvent Selection: Green Solvent Selection Guides. *Sustain. Chem. Process.* **2016**, *4*, 7. [CrossRef]
45. Ashry, E.S.H.E.; Rashed, N.; Abdel-Rahman, A.; Awad, L.F.; Rasheed, H.A. Synthesis of 2-Bromomethyl-3-Hydroxy-2-Hydroxymethyl-Propyl Pyrimidine and Theophylline Nucleosides Under Microwave Irradiation. Evaluation of Their Activity Against Hepatitis B Virus. *Nucleosides Nucleotides Nucleic Acids* **2006**, *25*, 925–939. [CrossRef]
46. Bafna, S.L.; Gold, V. 288. The Hydrolysis of Acetic Anhydride. Part II. Catalysis by Pyridine. *J. Chem. Soc.* **1953**, *288*, 1406–1409. [CrossRef]
47. Fersht, A.R.; Jencks, W.P. Acetylpyridinium Ion Intermediate in Pyridine-Catalyzed Hydrolysis and Acyl Transfer Reactions of Acetic Anhydride. Observation, Kinetics, Structure-Reactivity Correlations, and Effects of Concentrated Salt Solutions. *J. Am. Chem. Soc.* **1970**, *92*, 5432–5442. [CrossRef]
48. Bonner, T.G.; McNamara, P. The Pyridine-Catalysed Acetylation of Phenols and Alcohols by Acetic Anhydride. *J. Chem. Soc. B* **1968**, 795–797. [CrossRef]
49. *Handbook of Transnational Economic Governance Regimes*; Tietje, C., Brouder, A., Eds.; Martinus Nijhoff Publishers: Leiden, The Netherlands, 2009.
50. Ballesteros-Gómez, A.; Jonkers, T.; Covaci, A.; de Boer, J. Screening of additives in plastics with high resolution time-of-flight mass spectrometry and different ionization sources: Direct probe injection (DIP)-APCI, LC-APCI, and LC-ion booster. *Anal. Bioanal. Chem.* **2016**, *408*, 2945–2953. [CrossRef] [PubMed]
51. Zhang, T.; Ye, X.; Luo, X.; Niu, Z.; Wang, H.; Ma, Q. Simultaneous screening of 33 restricted substances in polymer materials using pyrolysis/thermal desorption gas chromatography–mass spectrometry. *Anal. Bioanal. Chem.* **2023**, *415*, 5463–5473. [CrossRef]
52. Liu, Y.; Hou, X.; Li, X.; Liu, J.; Jiang, G. Simultaneous determination of 19 bromophenols by gas chromatography–mass spectrometry (GC-MS) after derivatization. *Talanta* **2024**, *274*, 126015. [CrossRef] [PubMed]
53. Yang, H.; Luo, X.-J.; Zeng, Y.-H.; Mai, B.-X. Determination of tetrabromobisphenol-A/S and their eight derivatives in abiotic (soil/dust) samples using ultra-high performance liquid chromatography-tandem mass spectrometry. *J. Chromatogr. A* **2021**, *1647*, 462152. [CrossRef]
54. Xu, X.; Han, W. Analysis of tetrabromobisphenol A and bisphenol A in plant sample—method optimization and identification of the derivatives. *Environ. Sci. Pollut. Res.* **2023**, *30*, 82770–82779. [CrossRef]

Disclaimer/Publisher's Note: The statements, opinions and data contained in all publications are solely those of the individual author(s) and contributor(s) and not of MDPI and/or the editor(s). MDPI and/or the editor(s) disclaim responsibility for any injury to people or property resulting from any ideas, methods, instructions or products referred to in the content.